Title: The influence of anodic alumina coating nanostructure produced on EN AW-5251 alloy on type of tribological wear process

Author: Mateusz Niedźwiedź, Władysław Skoneczny, Marek Bara

Citation style: Niedźwiedź Mateusz, Skoneczny Władysław, Bara Marek. (2020). The influence of anodic alumina coating nanostructure produced on EN AW-5251 alloy on type of tribological wear process. "Coatings" (Vol. 10 (2020), iss. 2, art. no. 105, s. 1-9), doi: 10.3390/coatings10020105

coatings

MDPI

Article

The Influence of Anodic Alumina Coating Nanostructure Produced on EN AW-5251 Alloy on Type of Tribological Wear Process

Mateusz Niedźwiedź, Władysław Skoneczny * and Marek Bara

Institute of Materials Engineering, Faculty of Science and Technology, University of Silesia in Katowice, 40-007 Katowice, Poland; mateusz.niedzwiedz@us.edu.pl (M.N.); marek.bara@us.edu.pl (M.B.)

* Correspondence: wladyslaw.skoneczny@us.edu.pl; Tel.: +48-32-368563

Received: 11 December 2019; Accepted: 21 January 2020; Published: 24 January 2020

Abstract: The article presents the influence of the anodic alumina coating nanostructure produced on aluminum alloy EN AW-5251 on the type of tribological wear process of the coating. Oxide coatings were produced electrochemically in a ternary electrolyte by the DC method. Analysis of the nanostructure of the coating was performed using ImageJ 1.50i software on micrographs taken with a scanning electron microscope (SEM). Scratch tests of the coatings were carried out using a Micron-Gamma microhardness tester. The scratch marks were subjected to surface geometric structure studies with a Form TalySurf 2 50i contact profiler. Based on the studies, it was found that changes in the manufacturing process conditions (current density, electrolyte temperature) affect changes in the coating thickness and changes in the anodic alumina coating nanostructure (quantity and diameter of nanofibers), which in turn has a significant impact on the type of tribological wear. An increase in the density of the anodizing current from 1 to 4 A/dm^2 causes an increase in the diameter of the nanofibers from 75.99 ± 7.7 to 124.59 ± 6.53 nm while reducing amount of fibers from 6.6 ± 0.61 to 3.8 ± 0.48 on length 1 × 10^3 nm. This affects on a change in the type of tribological wear from grooving to micro-cutting.

Keywords: aluminum oxide layers; nanostructure; tribological wear

1. Introduction

Aluminum alloys are currently widely used in industry due to the low weight of the metal in relation to high mechanical strength and good thermal conductivity [1,2]. Due to the atmosphere, aluminum is automatically covered by a passive oxide coating a few nanometers thick, isolating the metal from contact with the environment [3]. However, in acidic or alkaline environments, the spontaneous oxide coating does not protect the metal well enough and aluminum corrosion occurs fairly quickly, leading to mass loss [4]. Therefore, ensuring proper protection of the aluminum surface involves the formation of an oxide coating of an appropriate thickness [5]. One method that allows adequate protection of aluminum alloys is electrochemical oxidation of the alloy surface. This process is called aluminum anodizing, and due to its properties that improve the hardness of metal, it is used on a large scale today [6]. Anodic alumina coatings in the electrochemical process can be formed using DC [7], constant voltage [8], pulse methods [9], and using AC [10], as well as AC imposed on DC [11]. Electrochemically produced oxide coatings have an amorphous structure [12]. The anodic alumina coating adopts a porous structure with vertically aligned cylindrical pores, depending mainly on the applied current density, electrolyte temperature, and aluminum alloy [13,14]. An important feature of anodic alumina coatings is their resistance to abrasive wear. This results in a wide application of anodized aluminum in friction pairs of engineering kinematic systems [15]. For this reason, tests are often carried out to assess the impact of the anodizing

parameters on the mechanical and tribological properties of oxide coatings [16]. One of the tests determining the mechanical properties of the coatings is the scratch test. Such tests allow one to not only determine the coefficient of friction value but also to determine the value of critical load causing damage to the coating [17,18]. In the first cited article, scientists investigated scratches of anodized aluminum in 10% oxalic acid at room temperature at 10–40 V. Subsequently, the crystal structure, chemical composition, surface morphology, and surface topography were examined. Studies have shown that higher anodizing potential leads to the formation of porous, thicker, and harder anodic alumina coatings. Anodized aluminum showed the formation of horizontal and vertical parallel cracks when attempting to scratch at a load of about 1 N. In the second article cited, researchers investigated the mechanical properties of AZ91 magnesium alloy coated with a double-layer Al_2O_3/Al. Mechanical properties were examined, among others, by a scratch test. It has been found that the mechanical properties of the coated alloy are significantly better, and the coating exhibits excellent adhesion to the substrate. Nanostructure studies are an important element of research related to the wear of oxide coatings and their adhesion to the substrate [19]. In the cited article, the authors started to produce Al_2O_3 layers by hard anodizing and thermo-chemical treatment. Then, they studied the microstructure, morphology, and tribological wear. Microstructure tests showed fiber sealing after physicochemical treatment, and it also increased the microhardness and polymer consumption during the tribological test. Our work focuses on the scratching of aluminum surfaces and anodic oxide coatings produced using various manufacturing parameters. In addition to the scratch resistance test, nanostructure analysis was performed to show the relationship between changes in the nanostructure and their impact on the type of tribological wear of the coatings which has not yet been studied. Scientists studied the nanostructure and friction of oxide layers in sliding running using finite elements [20]. They focused mainly on the oxidation of aluminum alloy for 60 min in an electrolyte consisting of sulfur and oxalic adipic acid at 298 K and a current density of 3 A/dm^2. The tribological properties of the oxide layer during reciprocating friction were tested using four different polymers (TG15, TGK20/5, TMP12, PEEK/BG). The highest wear and the highest friction coefficient were found for TMP12 material, while the lowest wear and friction coefficient for PEEK/BG. However, all cited articles lack reference to nanostructure for the type of tribological process, which makes our research innovative.

2. Materials and Methods

2.1. Research Material

The research material was anodic alumina coatings produced by an electrochemical method on the surface of plates made of EN AW-5251 aluminum alloy. This aluminum alloy is characterized by high mechanical strength and corrosion resistance. The chemical composition of the EN AW-5251 alloy (Table 1) allows one to easily modify its surface by anodizing.

Table 1. Chemical composition of the EN AW-5251 alloy.

Si	Fe	Cu	Mn	Mg	Cr	Ni	Zn	Ti	V	Other	Al
max 0.4	max 0.5	max 0.15	0.1–0.5	1.7–2.4	max 0.15	–	max 0.15	max 0.15	–	max 0.05	rest

Samples with an area of 0.1 dm^2 were subjected to etching using a 5% KOH solution (20 min) and a 10% HNO_3 solution (5 min). The temperature of the solutions was 296 K. The etching treatments ended with rinsing in distilled water. The sample surfaces (except for the reference sample) were modified by anodizing to form an anodic alumina coating on their surface using an electrochemical method. The surface of the samples was anodized by the DC method, using a GPR-25H30D power supply. During anodizing, a variable current density and electrolyte temperature were used to determine how the process parameters affect the type of tribological wear. A ternary electrolyte constituting an aqueous solution of 18% sulfuric acid (33 mL/L), oxalic acid (30 g/L), and phthalic acid (76 g/L) was used for the anodizing process. Anodic hard coatings produced in

electrolytes constituting of an aqueous solution sulfuric or oxalic acid require the use of low process temperatures (273–278 K). The addition of phthalic acid ensures that hard layers are obtained and enables the process to be carried out at room temperature. The anodizing process conditions are shown in Table 2.

Table 2. Anodizing process conditions.

Sample	Current Density j [A/dm^2]	Process Time t [min]	Electrolyte Temperature T [K]
A	1	20	283
B	1	20	293
C	4	20	313
D	4	20	283

After anodizing, the samples were rinsed in distilled water.

2.2. Research Methodology

The thickness of the anodic alumina coatings was measured by the contact method using a Fischer Dualscope MP40 instrument (Helmut Fischer GmbH+Co.KG, Sindelfingen, Germany) using the eddy-current method. Ten measurements were made (repeated 3 times) over the entire length of the sample, then the average values were calculated. Nanostructure tests of the oxide coatings were carried out on metallographic specimens using a Hitachi S-4700 scanning microscope (Hitachi, Tokyo, Japan) at 30,000x magnification. Anodic alumina coatings are non-conductive material, so they charge electrically when scanning through an electron beam, which prevents correct observation of the preparations. For better observation of the nanostructure, the samples were sputtered with carbon, which enables the discharge of electrons rebound during research. The micrographs were used for computer analysis of the image carried out using ImageJ 1.50i software. Using the image analysis procedures (smooth, bandpass filter, threshold), the number of fibers per nm and the diameter of the fibers were calculated. The scratch test was performed using a Micron-Gamma device (MicronSystema, Kiev, Ukraine). A Rockwell diamond indenter was used with a tip radius of 0.2 mm. A load of 4 ± 0.01 N was used during the test. The scratch marks were subjected to surface geometric structure (SGS) analysis. For this purpose, a Form TalySurf Series 2.50i profiler was used. The systematic scanning method was used on the transverse profile. The SGS parameters allowed the authors to determine the type of tribological wear.

3. Results and Discussion

Measurements of the thickness of the oxide coatings showed significant differences in the thickness depending on the anodizing conditions. Averaged values of measurements of the anodic alumina coating thickness together with deviations are presented in Table 3.

Table 3. Influence of anodizing conditions on thickness of oxide layers formed on EN AW-5251 aluminum alloy surface.

Sample	Oxide Layers Thickness d [μm]	Deviation [μm]
A	5.5	0.59
B	7.7	0.44
C	23.6	2.07
D	26.3	1.47

The current density as well as the electrolyte temperature during the anodizing process affects the thickness of the anodic alumina coatings. Considering the current dependence, one can notice a

significant increase in coating thickness at a constant electrolyte temperature and anodizing time together with an increase in current density (Samples A and D). An increase in the thickness of the coating along with an increase in current density (at a constant process time) is associated with an increase in electric charge. The anodic oxidation process, like any electrochemical process, proceeds according to Faraday's law, according to which a specific amount of electricity transforms aluminum into a specific amount of its oxide. Taking into consideration the temperature dependence at low current density values (Samples A and B), as the electrolyte temperature increases, the coating thickness increases. The increase in electrolyte temperature accelerates the migration of ions, which in turn increases the growth rate of the coating. However, at higher current density values (Samples C and D), the coating thickness decreases as the electrolyte temperature increases. Depending on the type of electrolyte in which the electrolysis process is carried out, a certain amount of produced Al_2O_3 is always dissolved by the electrolyte. In the thicker coatings, due to the resistance of the electrolyte column lying in the pores located between the oxide fibers, Joule's heat is released. The reduction in the Al_2O_3 layer thickness as the electrolyte temperature rises, at higher current densities, can therefore be attributed to the increasing secondary solubility of aluminum oxide associated with the higher electrolyte temperature.

Micrographs of the oxide coating nanostructures taken on metallographic specimens at 30,000x magnification (Figure 1) showed structure oriented along the direction of growth of the coating under the influence of an electric field.

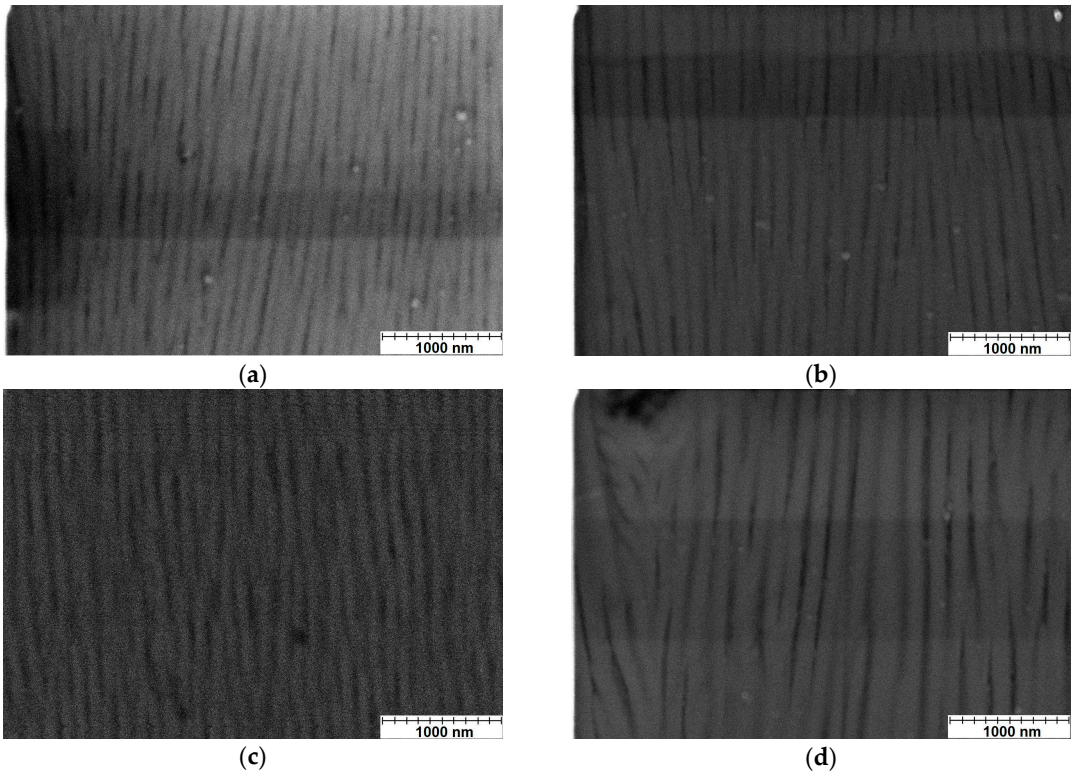

Figure 1. SEM micrograph (cross-section) of nanostructure of the coatings: (**a**) Sample A, (**b**) Sample B, (**c**) Sample C, (**d**) Sample D (sample designations as in Table 2).

In order to assess the impact of the coating production conditions on their nanostructure, the thickness and number of coating fibers were measured. For this purpose, each of the micrographs was subjected to image analysis, which enabled sharpening and visualization of the nanofibers. The first procedure used was the smooth function (first column), thanks to which the amount of noise in the images was significantly reduced. Then, the bandpass filter function (second column) was used, whose task was to filter the image in a banded way. The last function used was the threshold function with the dark back option selected (third column), thanks to which binarization of the

images was achieved—only black and white colors appear (the nanofibers are shown in black). The micrographs of the coatings after applying the appropriate procedures are shown in Figure 2.

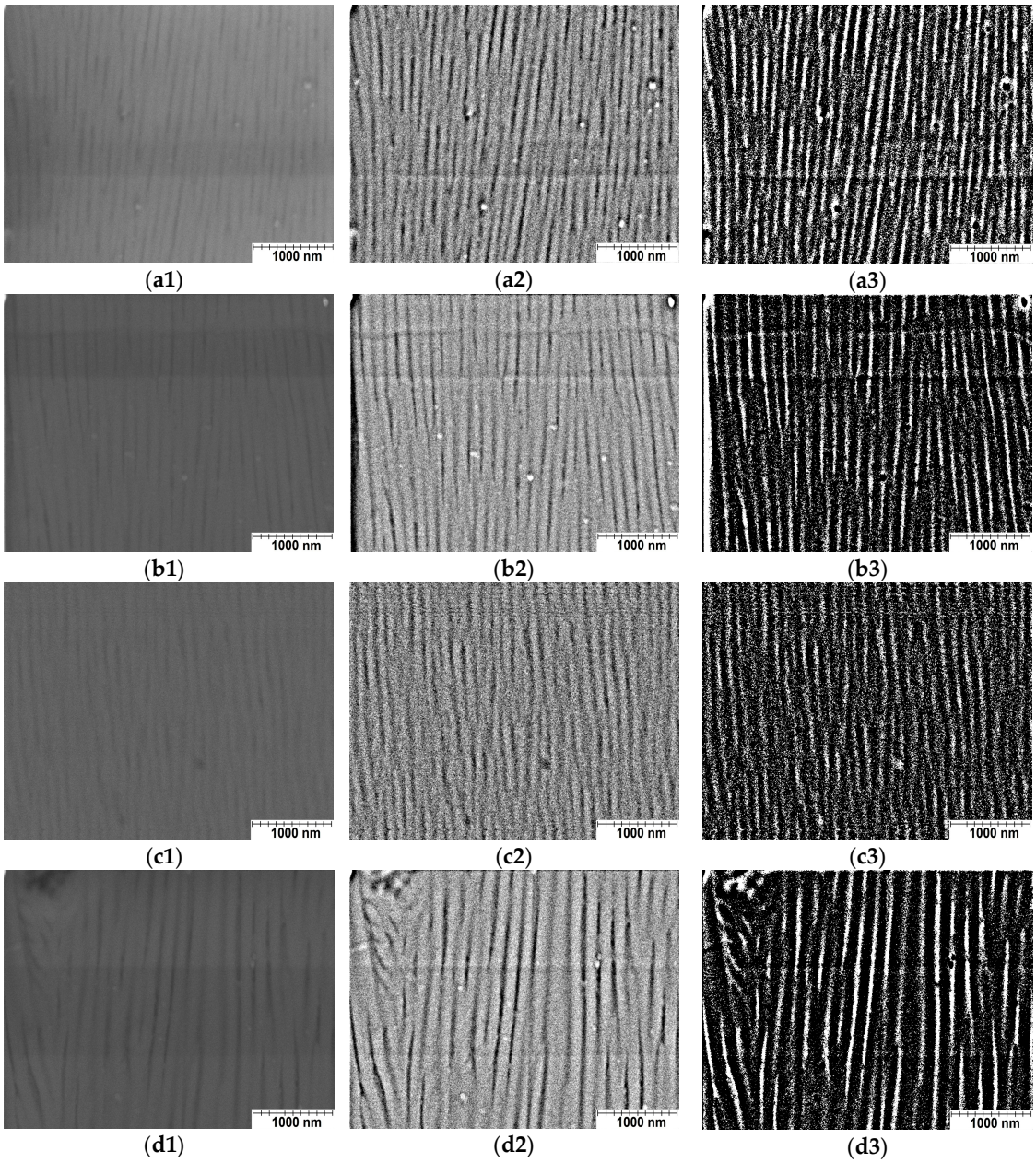

Figure 2. SEM micrograph (cross-section) of nanostructure of the coatings: (**a**) Sample A, (**b**) Sample B, (**c**) Sample C, (**d**) Sample D (sample designations as in Table 2), 1—image with smooth function, 2—image with bandpass filter function, 3—image with threshold function with dark back option selected.

The obtained results of the values of the aluminum oxide fiber diameters and the number of fibers on length 1×10^3 nm are presented in Table 4.

Table 4. Average values of diameters and number of coating fibers.

Sample	Amount of Fibers/nm ×10³	Deviation	Average Fiber Diameter [nm]	Deviation [nm]
A	6.6	0.61	75.99	7.70

B	5.1	0.52	92.52	6.48
C	5.8	0.57	101.87	8.06
D	3.8	0.48	124.59	6.53

The relationship between the coating thickness and the diameter of the aluminum oxide fibers is given by Equation (1).

$$y = 7.83x - 3.8, \quad (1)$$

y—coating thickness,
x—average fibers diameter.

On the basis of the image analysis data obtained from ImageJ 1.50i, histograms of the nanofibers with appropriate diameter groups in individual oxide coatings were made (Figure 3).

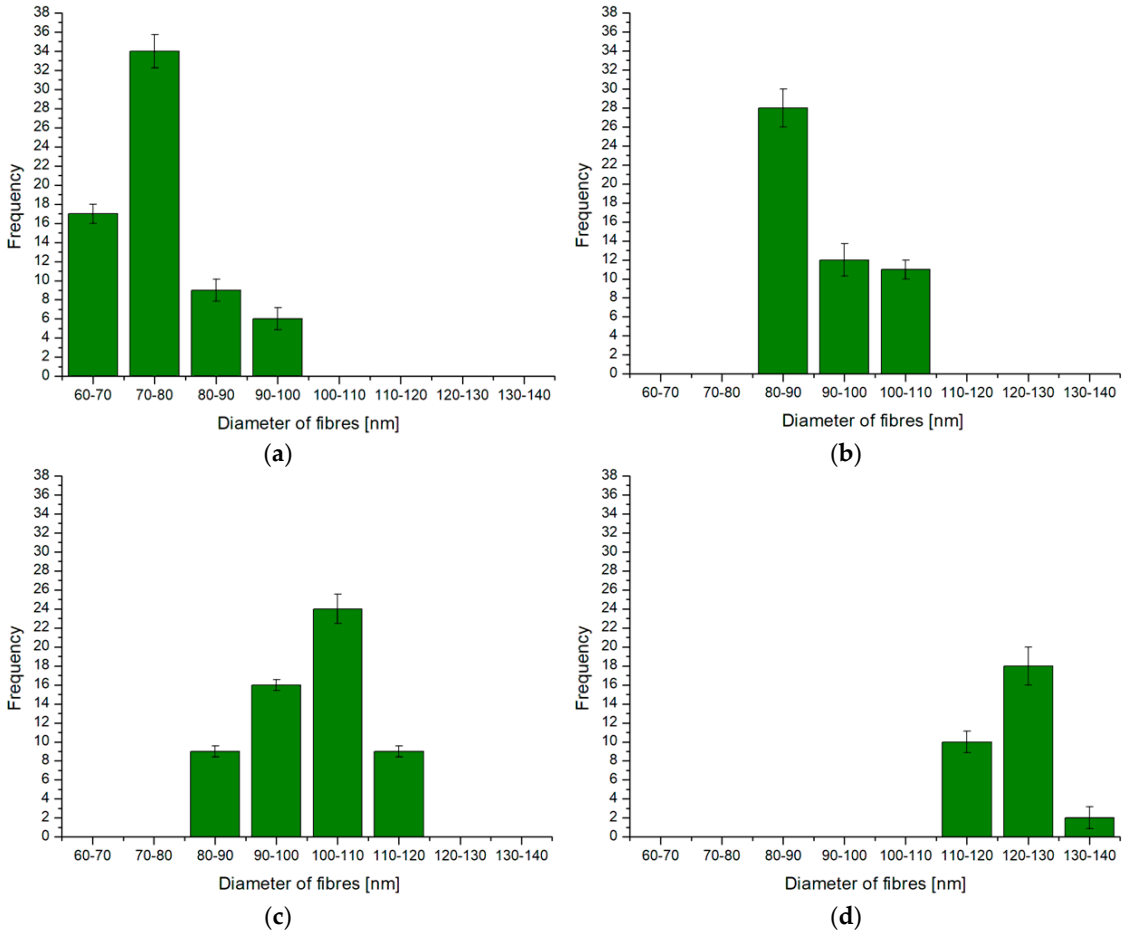

Figure 3. Histograms of nanofibers: (**a**) Sample A, (**b**) Sample B, (**c**) Sample C, (**d**) Sample D (sample designations in Table 2).

Computer analysis of the coating micrographs showed several significant relationships between the production parameters and the number of nanofibers and their diameters. For a constant current density of 1 A/dm^2, an increase in electrolyte temperature causes a decrease in the number of nanofibers per 1 × 10^3 nm while increasing their diameter (Samples A and B). In turn, at the current density of 4 A/dm^2 (Samples C and D), the increase in electrolyte temperature causes an increase in the number of nanofibers while reducing the diameter of the fibers. The above relationships most likely result from the increasing secondary solubility of aluminum oxide fibers with increasing temperature at higher current density values. At a constant electrolyte temperature,

an increase in current density (Samples A and D) causes a significant reduction in the number of nanofibers while increasing their diameter. Another important relationship is the linear relationship between the average diameter of the Al_2O_3 nanofibers coatings and the thickness of these coatings—an increase in the thickness of the oxide coating increases the diameter of the nanofibers. The coatings produced under extreme conditions (Samples A and D) with the largest and smallest thicknesses are also characterized by the largest and smallest number of nanofibers.

Figure 4 shows the transverse profiles of the surface of the oxide coatings and aluminum alloy made with the profiler after the scratch test. The area above the zero point is marked in green (material upsetting on both sides of the scratch), and in red the area after the scratch was made.

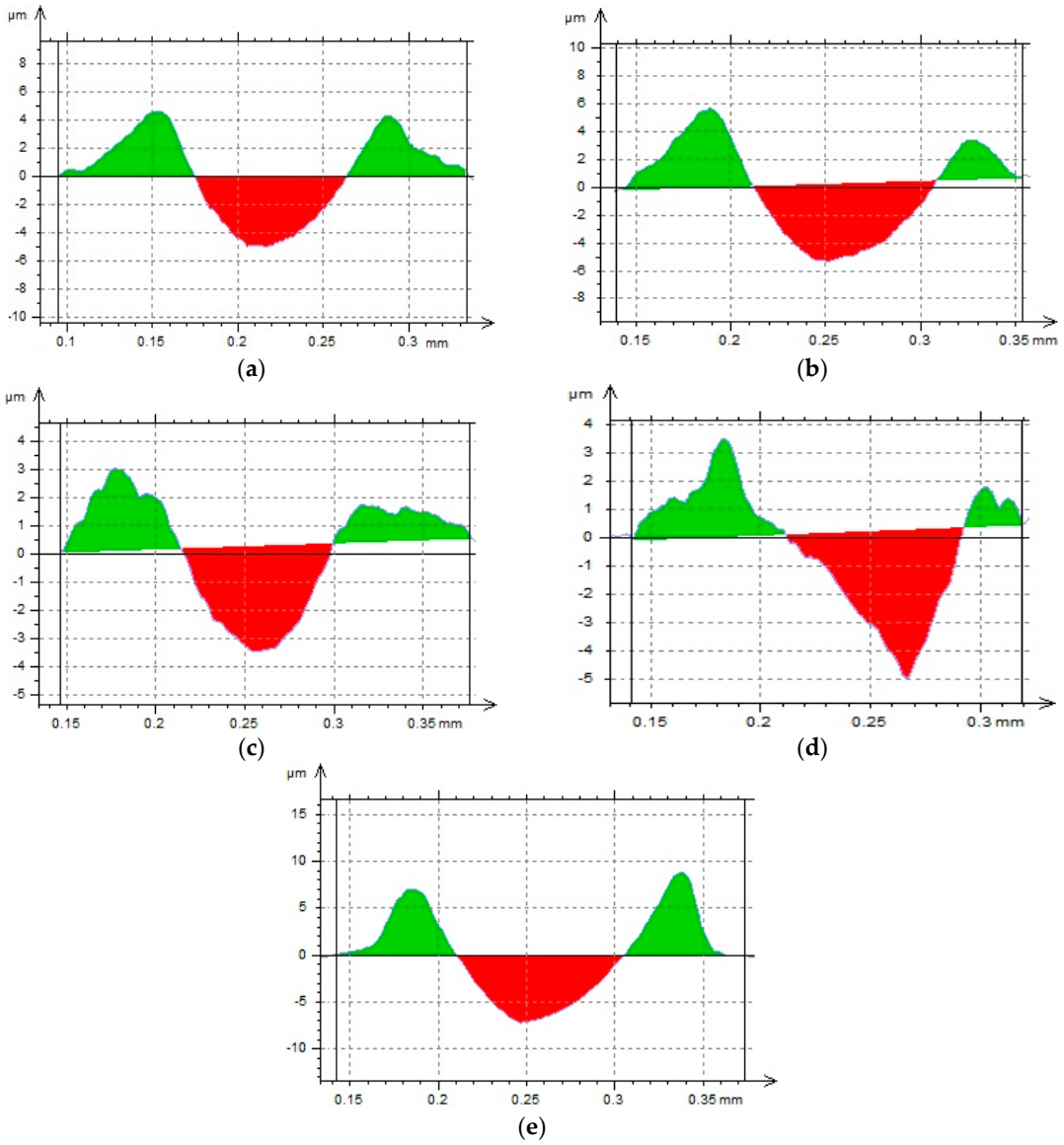

Figure 4. Transverse profiles of oxide coating and aluminum alloy surfaces after scratch test: (**a**–**d**): Sample designations in Table 2, (**e**): Aluminum alloy EN AW-5251.

The images showing the transverse profiles of the samples show areas both below and above the zero point, whose surface areas change depending on the coating production parameters. The shape of these areas also undergoes change. The aluminum alloy exhibited the most rounded area profiles. The increase in current conditions of the anodizing process leads to "sharpening" of the area profiles, which is caused by the increasing thickness of the oxide coatings and rising hardness. Table

5 shows the values of the ratio of the cross-sectional surface area of material upsetting around Scratch *f1* and the recess of Scratch *f2*. Based on these values, the processes of anodic alumina coating wear were determined.

Table 5. Values of ration of cross-sectional surface area of material upsetting around Scratch *f1* and recess of Scratch *f2*.

Sample	*f1*/*f2*	Deviation *f1*/*f2*	Wear Process
aluminum alloy	1.085	0.109	grooving
A	1.003	0.083	grooving
B	0.818	0.133	scratching, microcutting
C	0.753	0.230	scratching, microcutting
D	0.481	0.159	scratching, microcutting

Analysis of parameters *f1* and *f2* allowed the authors to determine the surface wear process of the tested samples. It was noticed that increasing the thickness of the anodic alumina coating (starting with pure aluminum) reduces the *f1*/*f2* dependence. As a result of the analysis, it was found that both in the case of pure aluminum and Sample A (smallest coating thickness) there is only plastic deformation of the surface layer, i.e., grooving. The tested surface is indented by the presence of unevenness or abrasive grain, which causes the material to move outside the surface. Grooving occurs if the value of the ratio $f1/f2 > 1$. In the remaining tested samples, there is scratching and microcutting, which in turn occurs in the case of $0 \leq f1/f2 \leq 1$. Roughness measurements carried out before the scratch test showed slight differences between layer surfaces. The Ra parameter value was 0.35 ± 0.035 μm. Slight differences in roughness do not affect the type of layer wear, however.

4. Conclusions

Based on the conducted research, it was found that the anodizing process parameters of the aluminum alloy EN AW-5251 surface affect the nanostructure of the anodic alumina coatings, whose construction, in turn, affects the type of tribological wear. An increase in current density while maintaining a constant electrolyte temperature results in the creation of an anodic alumina coating with a significantly increased diameter of coating nanofibers, while reducing their quantity. A linear relationship between the increase in the thickness of the oxide coating and the increase in diameter of the nanofibers was also demonstrated. A reduction in the *f1*/*f2* ratio value was also observed as the diameter of the nanofibers increased. From among the tested samples, only the surface of the aluminum alloy and anodic alumina coatings of the smallest thickness and the diameter of the nanofibers underwent grooving. The increase in production parameters, and hence the thickness of the coatings causes a change in the wear process of the coating from grooving to scratching and microcutting. Given the structure of the layers (fiber size, coating thickness depending on the density of the electric charge), the above studies are in line with previous scientific studies. Due to the fact that there is no literature research on the impact of nanostructure on the speed and mechanism of wear, we are not able to refer to literature.

Author Contributions: M.B. performed the analysis of the results; M.N. carried out the tests and wrote the manuscript; W.S. contributed to the concept and modified the manuscript. All authors have read and agreed to the published version of the manuscript.

Funding: This research received no external funding.

Conflicts of Interest: The authors declare no conflicts of interest

References

1. Davis, J.R. *Aluminum and Aluminum Alloys*; ASM International: Metals Park, OH, USA, 1993.
2. Davis, J.R. *Corrosion of Aluminum and Aluminum Alloys*; ASM International: Metals Park, OH, USA, 1999.

3. Lee, W.; Park, S.J. Porous anodic aluminum oxide: Anodization and templated synthesis of functional nanostructures. *Chem. Rev.* **2014**, *114*, 7487–7556.
4. Marcus, P.; Oudar, J. *Corrosion Mechanisms in Theory and Practice*; Marcel Dekker Inc.: New York, NY, USA, 1995.
5. Diggle, J.W.; Downie, T.C.; Goulding, C.W. Anodic oxide films on aluminum. *Chem. Rev*. **1969**, *69*, 365–405.
6. Runge, J.M. *The Metallurgy of Anodizing Aluminum—Connecting Science to Practice*, 1st ed.; Springer International Publishing: Cham, Switzerland, 2018.
7. Bara, M.; Kmita, T.; Korzekwa, J. Microstructure and properties of composite coatings obtained on aluminium alloys. *Arch. Metall. Mater.* **2016**, *61*, 1107–1112.
8. Michalska-Domańska, M.; Stępniowski, W.J.; Salerno, M. Effect of inter-electrode separation in the fabrication of nanoporous alumina by anodization. *J. Electroanal. Chem.* **2018**, *823*, 47–53.
9. Hsing-Hsiang, S.; Shiang-Lin, T. Study of anodic oxidation of aluminum in mixed acid using a pulsed current. *Surf. Coat. Technol*. **2000**, *124*, 278–285.
10. Fratila-Apachitei, L.E.; Duszczyk, J.; Katgerman, L. AlSi(Cu) anodic oxide layers formed in H_2SO_4 at low temperature using different current waveforms. *Surf. Coat. Technol*. **2003**, *165*, 232–240.
11. Posmyk, A. Co-deposited composite coatings with a ceramic matrix destined for sliding pairs. *Surf. Coat. Technol*. **2012**, *206*, 3342–3349.
12. Korzekwa, J.; Skoneczny, W.; Dercz, G.; Bara, M. Wear mechanism of Al_2O_3/WS_2 with PEEK/BG plastic. *J. Tribol*. **2014**, *136*, 1–7.
13. Fratila-Apachitei, L.E.; Tichelaar, F.D.; Thompson, G.E.; Terryn, H.; Skeldon, P.; Duszczyk, J.; Katgerman, L. A transmission electron microscopy study of hard anodic oxide layers on AlSi(Cu) alloys. *Electrochim. Acta* **2004**, *49*, 3169–3177.
14. Jia, Y.; Zhou, H.; Luo, P.; Luo, S.; Chen, J.; Kuang, Y. Preparation and characteristics of well-aligned macroporous films on aluminum by high voltage anodization in mixed acid. *Surf. Coat. Technol*. **2006**, *201*, 513–518.
15. Kmita, T.; Bara, M. Surface oxide layers with an increased carbon content for applications in oil-less tribological systems. *Chem. Process Eng*. **2012**, *33*, 479–486.
16. Kmita, T.; Skoneczny, W. Increase of operational durability of a plastic material-oxide coating couple as a result of the application of a pulsed anodizing process. *Eksploat. I Niezawodn.-Maint. Reliab*. **2010**, *45*, 77–82.
17. Choudhary, R.K.; Mishra, P.; Kaina, V.; Singh, K.; Kumar, S.; Chakravartty, J.K. Scratch behavior of aluminum anodized in oxalic acid: Effect of anodizing potential. *Surf. Coat. Technol.* **2015**, *283*, 135–147.
18. Xina, Y.; Huoa, K.; Hub, T.; Tanga, G.; Chu, P.K. Mechanical properties of Al_2O_3/Al bi-layer coated AZ91 magnesium alloy. *Thin Solid Films* **2009**, *517*, 5357–5360.
19. Kmita, T.; Szade, J.; Skoneczny, W. Gradient oxide layers with an increased carbon content on an EN AW-5251 alloy. *Chem. Process Eng*. **2008**, *29*, 375–387.
20. Kubica, M.; Skoneczny, W. The finite element method in tribological studies of polymer materials in tribo-pair with the oxide layer. *Tribol. Lett.* **2013**, *52*, 381–393.